

Validating a spatio-temporal model of observed neighborhood physical disorder

Jesse J. Plascak^{a,b,*}, Stephen J. Mooney^c, Mario Schootman^d, Andrew G. Rundle^e, Adana A.M. Llanos^{f,g}, Bo Qin^f, Chi-Chen Hong^h, Kitaw Demissieⁱ, Elisa V Bandera^f, Xinyi Xu^j

^a Comprehensive Cancer Center, The Ohio State University, Columbus, OH, United States of America

^b Division of Cancer Prevention and Control, Department of Internal Medicine, College of Medicine, The Ohio State University, Columbus, OH, United States of America

^c Department of Epidemiology, School of Public Health, University of Washington, Seattle, Washington, United States of America

^d Department of Clinical Analytics, SSM Health, St. Louis, MO, United States of America

^e Department of Epidemiology, Mailman School of Public Health, Columbia University, New York, NY, United States of America

^f Rutgers Cancer Institute of New Jersey, New Brunswick, New Jersey, United States of America

^g Department of Biostatistics and Epidemiology, School of Public Health, Piscataway, NJ, United States of America

^h Department of Cancer Prevention and Control, Roswell Park Cancer Institute, Buffalo, NY, United States of America

ⁱ Department of Epidemiology and Biostatistics, School of Public Health, SUNY Downstate Health Sciences University, Brooklyn, NY, United States of America

^j Department of Statistics, College of Arts and Sciences, Columbus, OH, United States of America

ARTICLE INFO

Keywords:

Built environment
Observed neighborhood physical disorder
Virtual neighborhood audit
Spatio-temporal universal Kriging
Perceived neighborhood physical disorder

ABSTRACT

This study tested spatio-temporal model prediction accuracy and concurrent validity of observed neighborhood physical disorder collected from virtual audits of Google Street View streetscapes. We predicted physical disorder from spatio-temporal regression Kriging models based on measures at three dates per each of 256 streetscapes ($n = 768$ data points) across an urban area. We assessed model internal validity through cross validation and external validity through Pearson correlations with respondent-reported perceptions of physical disorder from a breast cancer survivor cohort. We compared validity among full models (both large- and small-scale spatio-temporal trends) versus large-scale only. Full models yielded lower prediction error compared to large-scale only models. Physical disorder predictions were lagged at uniform distances and dates away from the respondent-reported perceptions of physical disorder. Correlations between perceived and observed physical disorder predicted from the full model were higher compared to that of the large-scale only model, but only at locations and times closest to the respondent's exact residential address and questionnaire date. A spatio-temporal Kriging model of observed physical disorder is valid.

1. Introduction

Neighborhood physical disorder is a health-related, built environment characteristic reflecting levels of public and private disinvestment, disrepair, and neglect (O'Brien et al., 2019). Evidence supports the existence of relationships between neighborhood physical disorder that is either independently observed or resident-perceived and various health behaviors or outcomes (O'Brien et al., 2019; South et al., 2018). For example, a recent randomized, controlled trial found that participants proximate to a remediated vacant lot reported lower psychological distress compared to residents proximate to vacant lots randomly selected to not receive remediation (South et al., 2018). Numerous

studies of neighborhood physical disorder and various health behaviors and outcomes including tobacco use, alcohol consumption, infant mortality, and obesity have also been conducted (see O'Brien et al., 2019).

A majority of studies have assessed participant-reported perceptions, as opposed to observed, neighborhood physical disorder for investigation with health behaviors and outcomes (O'Brien et al., 2019). Better characterization of observed neighborhood physical disorder could be beneficial despite the weight of evidence indicating that any potential causal effect on health due to observed neighborhood physical disorder acts through individual perceptions of disorder (O'Brien et al., 2019). Many studies of perceived neighborhood physical disorder and outcomes besides mental health have yielded mixed results (O'Brien et al.,

* Corresponding author at: Division of Cancer Prevention and Control, Department of Internal Medicine, College of Medicine, The Ohio State University, 1590 North High Street, Suite 525, Columbus, OH 43201, United States of America.

E-mail address: jesse.plascak@osumc.edu (J.J. Plascak).

<https://doi.org/10.1016/j.sste.2022.100506>

Received 30 April 2021; Received in revised form 27 December 2021; Accepted 22 March 2022

Available online 24 March 2022

1877-5845/© 2022 The Authors. Published by Elsevier Ltd. This is an open access article under the CC BY-NC-ND license (<http://creativecommons.org/licenses/by-nc-nd/4.0/>).

2019), raising concerns of same-source bias (Chum et al., 2019). Moreover, the growing ubiquity of publicly available, address-level streetscape images along with various virtual neighborhood audit tools and protocols allow for routine and resource-efficient assessment of observed neighborhood physical disorder without burdening study participants (Bader et al., 2015; Plascak et al., 2020; Rzotkiewicz et al., 2018).

Studies have taken advantage of widely-available virtual streetscapes to audit neighborhood physical disorder and build spatial models for estimation at locations associated with participants of epidemiologic studies (Mooney et al., 2017; Plascak et al., 2020; Remigio et al., 2019). These investigations demonstrate the utility of auditing locations unassociated with participants for the express intent of predicting levels of neighborhood physical disorder at study participant locations, without revealing study participant addresses to virtual streetscape providers (Bader et al., 2016). However, these studies have not modeled temporal relationships of observed neighborhood physical disorder, despite the existence of multiple image dates per some locations with dates as early as 2007 from the streetscape data source Google Street View (GSV) (Google).

Some studies have explored GSV streetscape date availability (Curtis et al., 2013; Fry et al., 2020; Nesoff et al., 2020; Tang and Long, 2019). Generally, these studies conclude that temporal variation in streetscape availability exists and should not be ignored. No study, however, has extended spatial models of observed neighborhood physical disorder by incorporating information on temporal dimensions in addition to spatial aspects. On the one hand, the unknown feasibility of constructing a spatio-temporal model of observed neighborhood physical disorder is an important gap because such a model could be used to estimate longitudinal exposures, therefore addressing a major limitation of epidemiologic studies relying on cross-sectional exposure data (Entwisle, 2007; O'Brien et al., 2019). On the other hand, observed neighborhood physical disorder may exhibit little temporal variation (Tang and Long, 2019), indicating that auditing repeated streetscapes across different times might be unnecessary and a poor use of resources. We tested the accuracy of a spatio-temporal model of observed neighborhood physical disorder and concurrent validity with perceived neighborhood physical disorder.

2. Materials and methods

2.1. Data

Neighborhood physical disorder observations were from two virtual audits of identical locations within Essex county, New Jersey (area = 315 km²). In both audits, trained raters used the virtual auditing platform CANVAS to assess GSV streetscapes for six attributes related to neighborhood physical disorder: presence of garbage (yes/no), presence of graffiti (yes/no), presence of abandoned buildings (yes/no), presence of dumpsters (yes/no), building conditions (very well-kept, moderately well-kept, fairly well-kept, poorly well-kept), and yard conditions (same scale as buildings) (Bader et al., 2015). The original audit included 7986 locations and took place from 11/27/2017 to 4/2/2018, as previously described (Plascak et al., 2020). The second audit took place from 1/29/2019 to 3/29/2019 and was a random subset of the first audit's locations. Raters of the second audit were divided into two teams of three based on streetscape dates accessed within GSV's timeline: current or historical (Google). The current team rated the GSV streetscape automatically returned from the GSV API, which is the most recent available at that location. The historical team was instructed to rate the oldest, 2009+ GSV streetscape. Images prior to 2009 were lower resolution, and excluded from rating to limit measurement error. The historical and current teams rated 957 and 798 locations, respectively. Audit responses were considered missing only if all six items had non-applicable responses (e.g., no buildings present, no residential yards present), leading to 7977 (99.9%), 869 (90.8%), and 769 (96.4%) valid

audit responses for the original, historical, and current audits, respectively. In order to maximize temporal variability in the audit data, we restricted all subsequent analyses to the 256 locations where a unique GSV streetscape date was available at an identical location for each of the three audits (original, historical, current) and responses were non-missing for all six neighborhood physical disorder indicators ($n = 768$, 2.44 date-locations per km²). Each team's audit data by location-date combinations are summarized in the Supplement. GSV streetscape dates ranged from June 2009 to October 2018.

Respondent-reported perceptions of neighborhood physical disorder were from a breast cancer survivor cohort with spatial and temporal extents overlapping that of the virtual audits (Bandera et al., 2020; Plascak et al., 2020). Briefly, Black women between the ages of 20–75 years, diagnosed with breast cancer while a resident of one of ten New Jersey counties were eligible to participate (Bandera et al., 2020). Participants' geocoded residential address was obtained through linkage with New Jersey State Cancer registry files. Participants were administered the Ross and Mirowsky perceived neighborhood physical disorder questionnaire approximately 24 months following diagnosis (Ross and Mirowsky, 1999). The questionnaire assesses agreement – strongly agree, somewhat agree, neither agree nor disagree, somewhat disagree, strongly disagree – on each of six statements specific to a respondent's neighborhood: 'is clean', 'people take good care houses/apartments and yards', 'there is a lot of graffiti', 'is noisy', 'vandalism is common', 'a lot of abandoned/boarded up buildings'. 'Neighborhood' was defined for participants as, 'the general area around your house where you might perform routine tasks, such as shopping, going to the park, or visiting with neighbors'. The neighborhood perception questionnaire was administered to 116 Essex county participants, whose residential spatial distribution is concentrated in the Southeast of the county (Plascak et al., 2020). We further restricted to participants with the most accurate geocodes (i.e., using street address and zip code, $n = 112$), survey dates no later than 4 months prior to the latest GSV streetscape date (June 2018, $n = 61$), and non-missing perceived neighborhood physical disorder responses ($n = 58$). We performed the temporal restriction in anticipation of calculating time-lagged correlations between Kriging-predicted audited neighborhood physical disorder and perceived neighborhood physical disorder that would not be off-support and to retain the same participants within each lagged correlation. Without this temporal restriction, levels of neighborhood physical disorder would have been predicted at months occurring after the latest audited GSV streetscape date; especially among participants enrolled later in the study. The first two perceived neighborhood physical disorder items were reversed and item responses were sum scored upon finding adequate internal consistency reliability (Cronbach's alpha = 0.85) (Pruitt et al., 2012).

2.2. Statistical analysis

An audited neighborhood physical disorder score was estimated at each location-date combination using item response theory analysis of the six audit items (Mooney et al., 2017). Total area under the information curve was 0.96 indicating adequate internal consistency reliability (Thissen, 2000). A spatio-temporal regression Kriging model was built to predict audited neighborhood physical disorder at locations across Essex County and times ranging from June 2009 and October 2018, including at dates and locations of the 58 participants with self-reported perceived neighborhood disorder responses. Regression Kriging allowed direct comparison of model validity metrics between the large-scale and small-scale trend components.

Audit rater variability – that is, individual raters' tendency to assess disorder indicators in consistently different ways – can be considered systematic measurement error and accounted for statistically (Hoeben et al., 2018). To account for audit rater variability, we first regressed audited neighborhood physical disorder scores on raters using a series of dummy variables for raters within a linear regression (p-value of Type III F-test < 0.0001). The residuals of this regression ranged from –1.88 to

2.61 (standard deviation = 0.750, interquartile range = 0.951), represent rater-adjusted neighborhood physical disorder scores (hereafter, ‘observed neighborhood physical disorder’), and were used in all subsequent analyses.

The spatio-temporal distribution of observed neighborhood physical disorder was summarized in trellis plots. Satisfaction of the spatio-temporal stationarity assumption was investigated through a linear regression model of observed neighborhood physical disorder with spatial and temporal indices as covariates. Third order polynomials were considered for spatial and temporal indices and covariates were retained in the model if 95% confidence intervals were sufficiently narrow. Spatial and temporal covariates were mean centered to reduce collinearity between polynomial terms. The linear model indicated large-scale spatial but not temporal trends in observed neighborhood physical disorder. Model residuals, ϵ , represent observed

$$\text{Observed neighborhood physical disorder} = 0.093 + 0.117(\text{latitude}) + -0.007(\text{latitude}^2) + -0.001(\text{latitude}^3) + -0.038(\text{longitude})$$

$$+ -0.003(\text{longitude}^2) + -0.008(\text{latitude} * \text{longitude}) + \epsilon$$

physical disorder values that were free from large-scale trend but were further tested for smaller-scale spatio-temporal patterns.

An empirical spatio-temporal variogram was built limiting the spatial separation of data pairs to 8 km, temporal separation to 1600 days, and assuming irregular data collection and semivariogram binning (see Fig. 2 for evidence of irregularity and spatio-temporal extents of data). A theoretical spatio-temporal semivariogram was fit according to a simple sum metric model family which allows for variogram components that are spatial, temporal, joint spatio-temporal, and a joint spatio-temporal nugget (Pebesma and Heuvelink, 2016). The theoretical semivariogram model was fit by eye; nugget, partial sill, range parameters and functional form (e.g., exponential, spherical, circular, etc.) were best fit visually. Plots of empirical semivariograms, theoretical semivariograms, and the difference between empirical and theoretical were produced. The best fitting theoretical semivariogram was considered that which yielded the smallest differences between the empirical and theoretical semivariograms within the estimated ranges of the spatial and temporal parameters; larger differences between the two semivariograms beyond the estimated ranges were de-emphasized in visual model fitting because any observations beyond these range values would contribute relatively little information to subsequent Kriging predictions. Global, spatio-temporal Kriging using the fitted theoretical semivariogram and observed neighborhood physical disorder values was used to predict the small-scale neighborhood physical disorder, ϵ from the equation above, at gridded locations across the study area every 6 months between August 2010 and August 2018. An overall prediction of neighborhood physical disorder was calculated by adding predictions from the Kriging model and large-scale trend model at the gridded locations and dates. Results were mapped.

Validity was assessed through 10-fold cross validation and a matrix of Pearson correlations between model-predicted neighborhood physical disorder and perceived neighborhood physical disorder. Cross validation prediction accuracy was measured by averaged root mean square error (RMSE), normalized RMSE (i.e., RMSE divided by observed neighborhood physical disorder IQR), and coefficient of determination (R^2) from each fold. Thus, 10 Kriging models were built, each one using 90% of the data and used to predict responses to the 10% of data left out within each fold. The fitted theoretical semivariogram calculated using the full data was used in each of the 90% training datasets.

The correlation matrix was composed of temporal and spatial lags based on set times and distances away from each respondent’s actual residence (spatial lag = 0) and date of survey completion (time lag = 0). Each temporal and spatial lag represented 1 month and 0.1 km of separation, respectively. Number of total temporal lags ($n = 42$) and spatial lags ($n = 36$) were based on the ranges estimated from theoretical semivariograms and limited to locations and times that were within the extents of the audit data to ensure on-support predictions. To account for potential variability of the two spatial dimensions – latitude and longitude – that factor into the calculations between actual and lagged distances, 16 locations were generated per each respondent-lag combination. The 16 locations were uniformly distributed around a circle with radius equal to the lagged distance of the matrix. Thus, a total of 1366,596 predictions of observed neighborhood physical disorder were calculated using the linear regression and full global spatio-

temporal Kriging models described above (58 respondents | spatial lag = 0 × 42 temporal lags + (58 respondents × 35 spatial lags × 16 locations per spatial lag × 42 temporal lags)). Respondents’ 58 perceived neighborhood physical disorder values were replicated across each of the 1512 cells of the matrix. A similar correlation matrix was calculated using observed neighborhood physical disorder predictions from the large-scale only model (equation above). To highlight the spatio-temporal lags where observed physical disorder predictions from the full model might be more valid than those predictions from the large-scale only model, we subtracted correlation coefficients of the large-scale only from the full model. We expected the highest correlations between predicted and perceived neighborhood physical disorder to occur at or near time and spatial lag of zero, and correlations to decrease as a function of lags away from zero. Data were projected equidistant conic. Analyses were conducted in SAS 9.4, ArcMap 10.6 and R v4.0.4 primarily with the gstat package v2.0–6 (Environmental Systems Research, 2020; Pebesma and Heuvelink, 2016; Sas, 2014; Team, 2013).

3. Results

3.1. Spatio-temporal data description and semivariograms

Availability of locations and dates with non-missing, observed neighborhood physical disorder data appear spatio-temporally structured, with a greater proportion of data available in the Southeast of the study region and between May and October (Fig. 1). The sample lacked any data between December and April of any year, lacked any data from 2010 or 2011, and only a few data points in 2009 or 2014. Higher observed neighborhood physical disorder values also appear to be concentrated in the Southeast as indicated by the warmer colors of both Fig. 1 and Fig. 2, which displays the modelled large scale spatial trend of observed neighborhood physical disorder.

The empirical and fitted theoretical semivariograms of de-trended observed neighborhood physical disorder suggest spatial and temporal autocorrelation; albeit with a temporal partial sill that is much smaller than the spatial partial sill (Fig. 3). Spherical theoretical semivariograms were fit to all three variogram components (spatial, temporal, joint) based on the following parameters: spatio-temporal nugget = 0.1, spatial partial sill = 0.35, spatial range = 2.1 km, temporal partial sill = 0.03, temporal range = 900 days, joint spatio-temporal partial sill = 0.001, joint spatio-temporal range = 0.005, and spatio-temporal anisotropy=0.001. There seem to be slight wave patterns in semivariance across space and time with a decrease in semivariance at

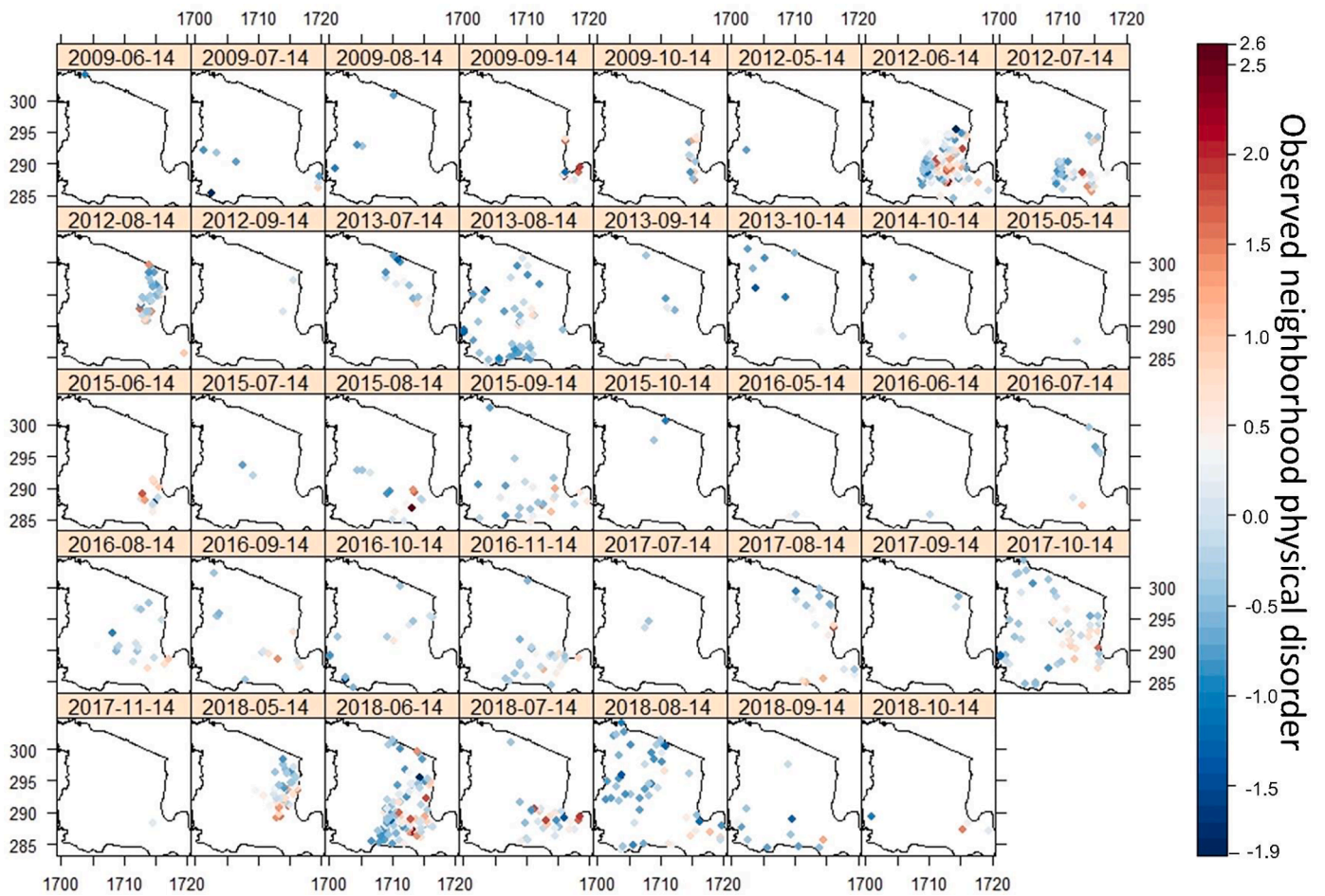


Fig. 1. Observed neighborhood physical disorder values by location and date, Essex County, New Jersey, $n = 768$.

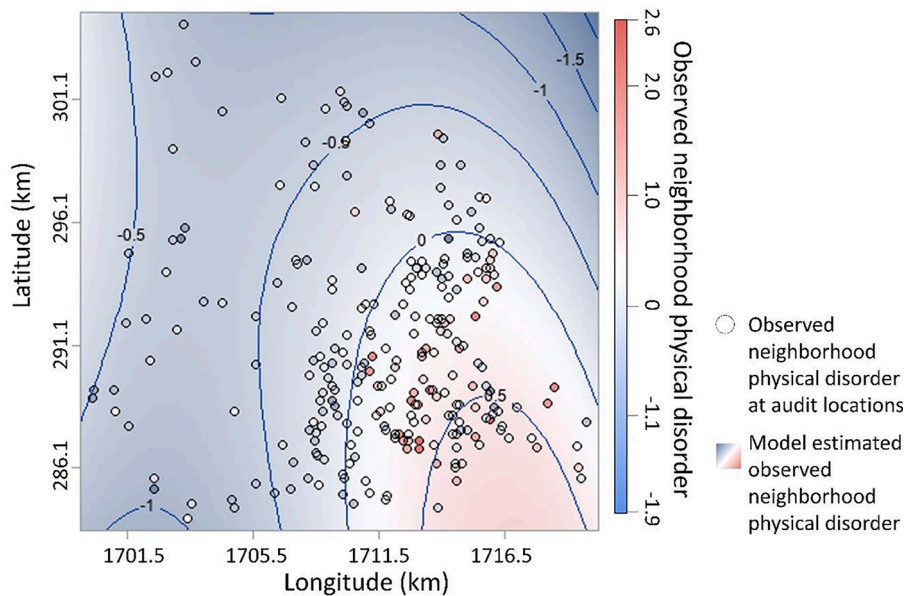


Fig. 2. Estimated observed neighborhood physical disorder from a model of large-scale trend, Essex County, New Jersey, $n = 768$.

distances beginning around 5–6 km and times between 400 and 800 days. Semivariance appears to also dip again at times beyond the estimated range of 900 days. These trends are clearer when subtracting the empirical from theoretical semivariograms (Fig. 4). The theoretical

semivariogram is overestimating semivariance (i.e., underestimating correlation) between pairs of points separated by distances and times indicated by darker shades of red in Fig. 4; our theoretical semivariogram estimates larger differences than we observe from the data

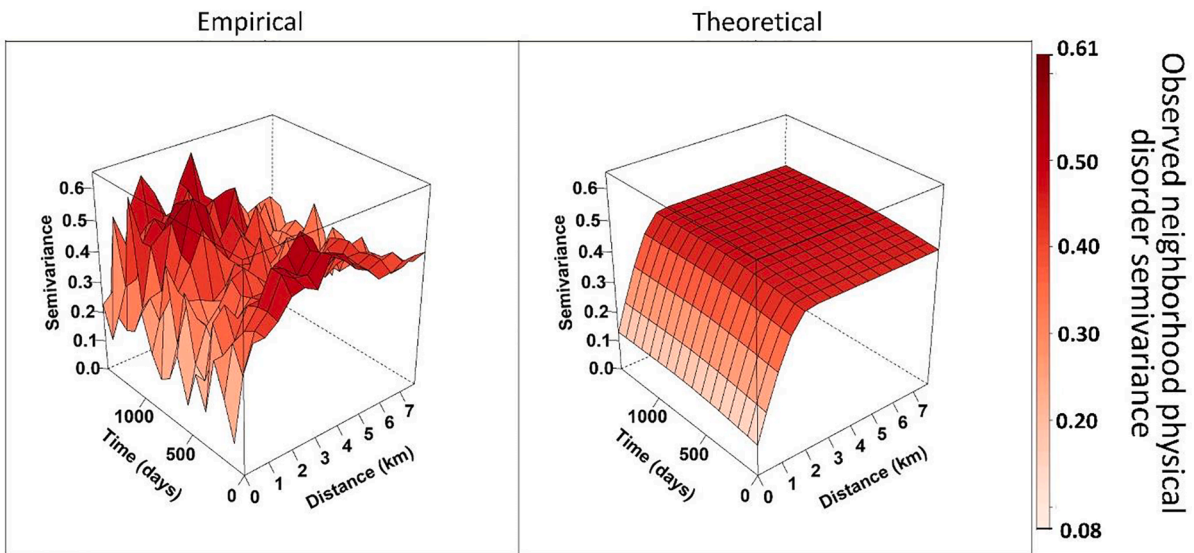


Fig. 3. Empirical and fitted theoretical spatio-temporal semivariograms of observed neighborhood physical disorder, Essex County, New Jersey, $n = 768$.

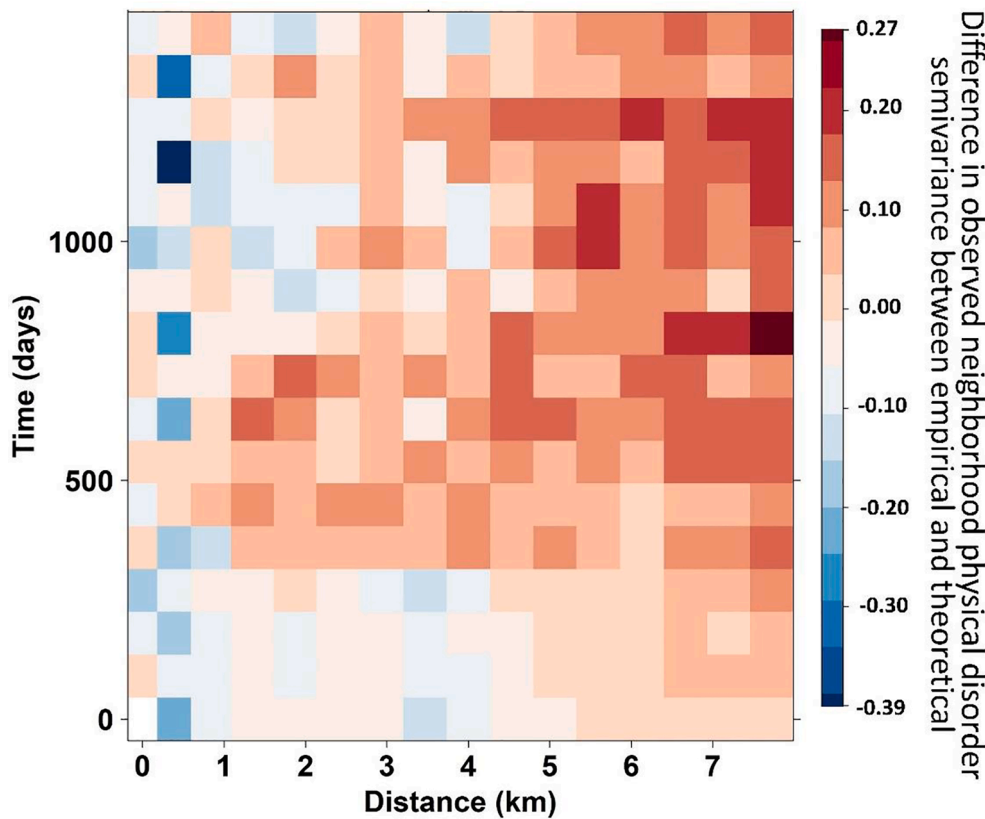


Fig. 4. Differences between empirical and fitted theoretical spatio-temporal semivariograms of observed neighborhood physical disorder, Essex County, New Jersey, $n = 768$.

between pairs of points separated by these distances and times. Conversely, semivariance is underestimated between pairs of points separated by distances and times indicated by shades of blue; our theoretical semivariogram estimates smaller differences than we observe from the data between pairs of points separated by these distances and times. Light red colors represent point pairings with little difference between empirical and theoretical semivariograms; our theoretical semivariogram estimates similar differences to what we observe from the data between pairs of points separated by these

distances and times. These light red colors are clustered around short times and distances where nearby points will have the greatest weight in Kriging predictions; data points with the largest weights will have the least covariance error in Kriging predictions.

3.2. Observed neighborhood physical disorder predictions and model validity

Neighborhood physical disorder estimated from the sums of the

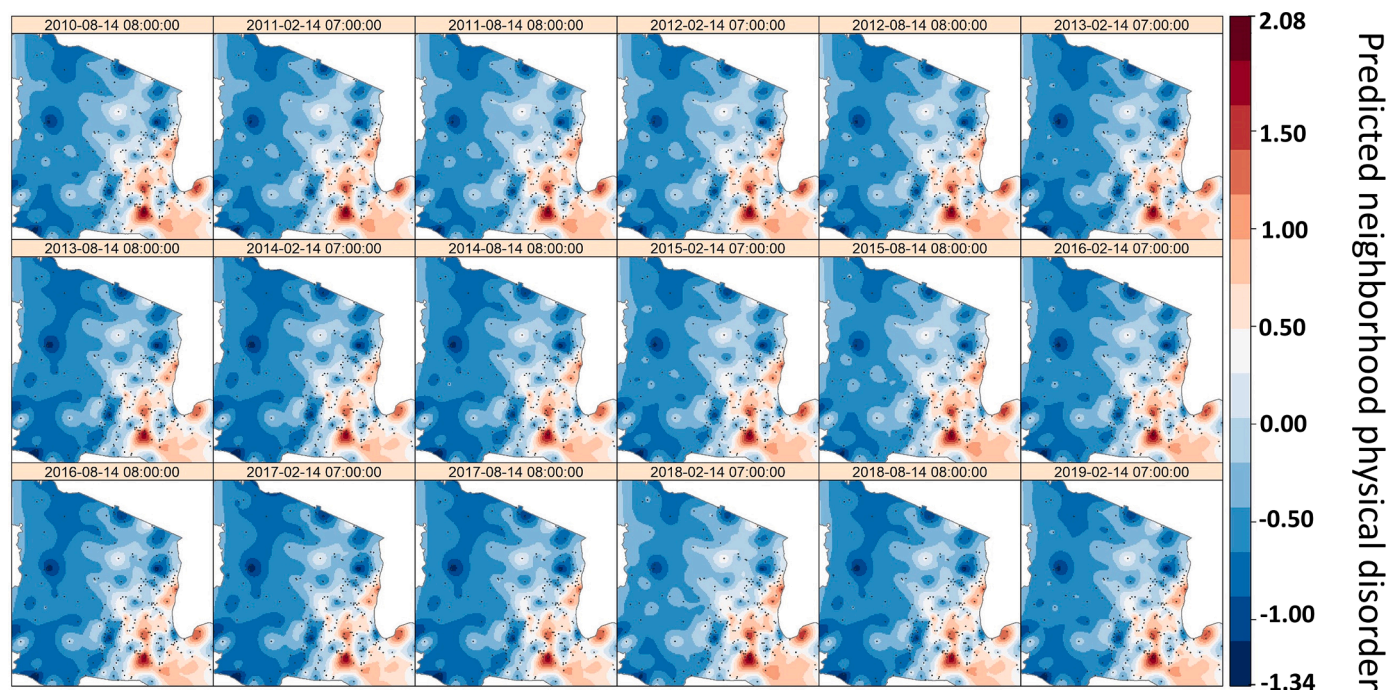


Fig. 5. Predicted observed neighborhood physical disorder across Essex County, New Jersey 2010–2018.

Table 1

Accuracy results from 10-fold cross-validation comparing observed neighborhood physical disorder predictions from large-scale only to combined large- and small-scale models, Essex County, New Jersey, $n = 768^1$.

	RMSE	IQR	NRMSE	R ²
Large-scale trend only	0.418	0.951	0.439	0.272
Combined large- and small-scale spatio-temporal trends	0.209	0.951	0.220	0.632

¹ RMSE = averaged root mean square error; IQR = interquartile range of observed neighborhood physical disorder; NRMSE = normalized root mean square error; R² = averaged coefficient of determination.

predictions from the linear regression and spatio-temporal Kriging models suggest general trends of higher neighborhood physical disorder in the Southeast of Essex County that is largely stable over time (Fig. 5). RMSE and NRMSE from combined large- and small-scale models was half of the RMSE and NRMSE from the large-scale only model (Table 1). Similarly, R² was more than twice as large comparing the combined large- and small-scale trend models to the large-scale only model. The improved accuracy of combined predictions is further demonstrated when analyzing correlation matrices of perceived neighborhood physical disorder and model-predicted neighborhood physical disorder by time and space lags (Fig. 6 and Supplement Figures). The highest correlations are at temporal and Fig. 5. Predicted observed neighborhood physical disorder across Essex County, New Jersey 2010–2018

¹ Observed neighborhood physical disorder at time lag 0 indicates a model prediction at the exact date when perceived neighborhood physical disorder was assessed. Negative time lags indicate observed neighborhood physical disorder values predicted at times occurring before the date when perceived neighborhood physical disorder was assessed. Positive times indicate observed neighborhood physical disorder values predicted at times occurring after the date when perceived neighborhood physical disorder was assessed. Distance at lag 0 indicates that observed neighborhood physical disorder was predicted at the exact address where perceived neighborhood physical disorder was assessed. Distances > 0 indicate observed neighborhood physical disorder values estimated at locations 'X km' away from the address where perceived neighborhood physical disorder was assessed. 16 different locations

were selected along an arc with radius = distance_x. The 16 locations were uniformly distributed along the arc and all points were within the study region. Correlations were then calculated under a multiple imputation framework where correlations from the 16 distance realizations were considered an imputed dataset (distance lag of 0 contain no imputation realizations). Correlation coefficient differences were from two sets of correlations: those using predictions of observed physical disorder from the full model and those using predictions of observed physical disorder from the large-scale only model. spatial lags closest to zero (i.e., respondent's exact questionnaire date and residential address) when predicting observed neighborhood physical disorder from the combined large- and small-scale models (Supplement Figure a). Correlations between perceived and model-predicted neighborhood physical disorder when using predictions limited to the large-scale model are also highest at spatial lags closest to zero but constant across temporal lags, as expected due to a lack of time covariates in the large-scale regression equation above (Supplement Figure b). Comparing the matrices by subtracting correlation coefficients of the combined large- and small-scale models by those of the large-scale only indicates the lags at which model-estimated observed neighborhood physical disorder from the full model more strongly correlate with perceived neighborhood physical disorder (red colors Fig. 6). Taken as a measure of observed neighborhood physical disorder concurrent validity, the predictions from the combined models exhibit superior validity at any time lags with separation distances less than 0.5 km. Observed neighborhood physical disorder predictions from the large-scale only model, however, indicate greater validity at all time lags with separation distances greater than 0.5 km. The spatial versus temporal variability in neighborhood physical disorder is also highlighted in the vertical and horizontal gradients of Supplement Figure a; the gradient left to right indicates that disorder varies strongly over space whereas the markedly smaller vertical gradient indicates that disorder varies much less over time.

4. Discussion

The full, spatio-temporal regression Kriging model which accounted for both large- and small-scale patterns in observed neighborhood

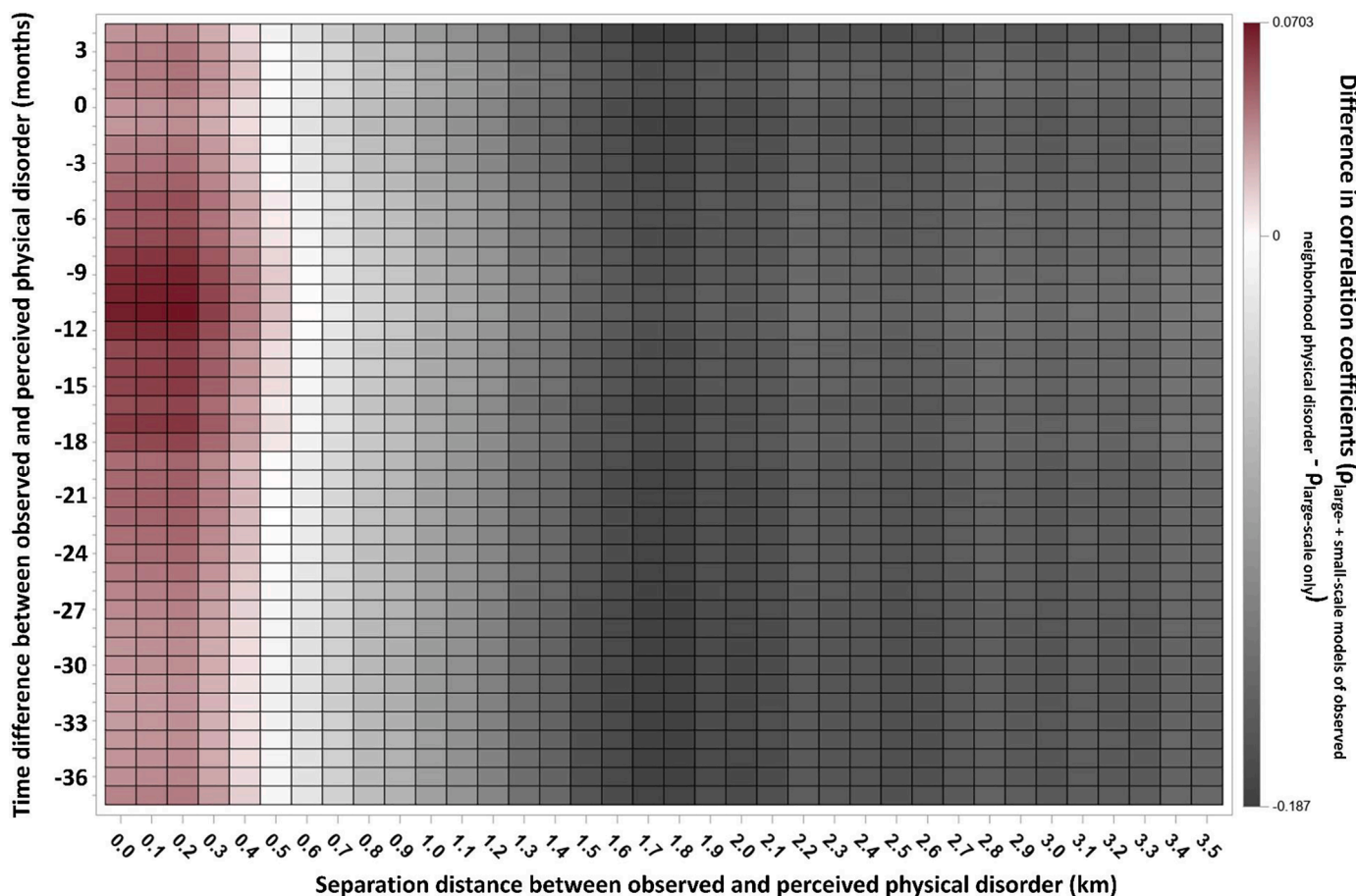


Fig. 6. Differences in correlation coefficients of perceived neighborhood physical disorder and predicted neighborhood physical disorder by time and space lags¹.

physical disorder exhibited substantially greater accuracy compared to the model that accounted only for large-scale patterns. Observed-perceived neighborhood physical disorder correlations resulting from the full spatio-temporal model are highest among predictions of observed disorder nearest to the address and survey date when perceived disorder was self-reported. Together this provides evidence for the general validity of a spatio-temporal regression Kriging model of observed neighborhood physical disorder and suggests that information on spatial and temporal indices of audits can yield greater prediction accuracy than spatial-only models. Moreover, its general stability over time suggests that long-term exposure to objective neighborhood physical disorder might be an important consideration in epidemiologic studies.

4.1. Utility of collecting spatio-temporal dimensions of observed neighborhood physical disorder

Observed-perceived neighborhood physical disorder correlations resulting from the full spatio-temporal model are slightly higher compared to those of the large-scale only model among predictions of observed disorder nearest to the address when perceived disorder was reported. In contrast, observed-perceived neighborhood physical disorder correlations among predictions of observed disorder that are further away from the address where perceived disorder was reported (> 0.5 km) are higher when predicted from the large-scale only model compared to the full spatio-temporal regression Kriging model. Assuming these correlations represent a true and generalizable measure of validity, the choice to collect and develop a spatio-temporal regression Kriging or a simpler spatial trend regression model to yield neighborhood physical disorder predictions at locations and times relevant for

a specific epidemiologic dataset could be guided by the precision of the spatial and temporal indices of that epidemiologic data. For example, a study of the correlation between observed neighborhood physical disorder and health among participants with a residential address geocoding error of > 0.5 km might yield more accurate correlations if observed neighborhood physical disorder were estimated from a model accounting for large-scale spatial trends only. Similarly, a study linking model-predicted observed neighborhood physical disorder to a dataset that only provides participants' zip code tabulation area of residence (e.g., Behavioral Risk Factor Surveillance System) might be better off building a simple model of neighborhood physical disorder that is a function of polynomials of the x and y coordinates knowing that, in the U.S., zip code tabulation areas have a median area of 96 km (radius of 5.5 km if a circle) (Donaldson, 2013). In contrast, it might be advisable to collect and model the spatio-temporal dependencies of observed neighborhood physical disorder within studies that collect residential addresses and geocode those addresses to a latitude and longitude with high precision (e.g., high quality cancer registries).

4.2. Patterns of perceived and observed neighborhood physical disorder correlations

As hypothesized, correlations between perceived and observed neighborhood physical disorder predicted from either model were highest where data were spatially nearest one another and gradually decreased as a function of spatial separation between data. This is in line with previous studies demonstrating that individuals perceive their neighborhoods as having spatial boundaries (Donaldson, 2013; Taylor, 2012). In contrast to the expected spatial trends, the highest correlations between perceived and observed neighborhood physical disorder were

not when data were temporally nearest (i.e., assessed at identical dates), but when observed neighborhood physical disorder was predicted approximately 9–12 months prior to the dates when residents reported perceived neighborhood physical disorder. Compared to previous research on residents' perceptions of neighborhood spatial boundaries, far less is known of timeframes recalled by residents when prompted to characterize specific attributes of their neighborhood (Taylor, 2012). A systematic review of temporal variation in physical activity found that physical activity was highest during summer months and lowest in winter months among regions with temperate climates, which was attributed to residents interacting outdoors more often during favorable weather (Tucker and Gilliland, 2007). It is possible that the timeframe recalled by residents when reporting neighborhood physical disorder perceptions coincides with outdoor neighborhood activities – walking within the neighborhood, interacting with neighbors, engaging in home/yard maintenance, etc. – that are more likely to occur in warmer months. If true, the temporal pattern between perceived and observed neighborhood physical disorder correlations could reflect the inclination to recall the previous summer's neighborhood characteristics and the months when residents reported neighborhood physical disorder perceptions. Indeed, the average time between when residents reported neighborhood perceptions and the previous July (summer in the Northern hemisphere) was 5.9 months. Future studies should specify an exact recall timeframe within neighborhood perception questions which would help align the temporal indices of observed and resident-perceived neighborhood physical disorder measures. Such spatio-temporally aligned measures could lead to better understanding of how observed neighborhood factors might impact perceptions and eventually health and well-being (Entwisle, 2007; O'Brien et al., 2019).

4.3. Limitations

Limitations of this study include reliance on GSV for observed neighborhood physical disorder characteristics; unclear generalizability among areas that are less urban, non-sampled dates, different populations, and health behaviors and outcomes; and modest sample sizes of audit and self-report data used for validation. Limitations to using GSV for neighborhood audits were discussed at length elsewhere (Bader et al., 2015; Curtis et al., 2013; Plascak et al., 2020), but highly relevant for this study is the potential for differential data availability by location and date. GSV streetscapes used to build the model were sparsely available or absent between fall-early spring seasons; 2009–2011 and 2014; and in the west of the county where the population is less dense. While Google's proprietary, image capture protocol is unclear, a 2013 study reported similar urban-rural and temporal variation in streetscape availability (Curtis et al., 2013), which appears to have persisted despite several years of additional data. The effect of spatio-temporally patterned data availability should minimally impact results of this study due to various reasons: 1) observed neighborhood physical disorder is considered an urban construct; (Sampson and Raudenbush, 1999) 2) model-estimated neighborhood physical disorder was strongly driven by spatial versus temporal model components, and 3) the spatio-temporal extents of perceived disorder data largely overlapped that of the audit data. Similarly, generalizability of these results to less densely populated regions, winter months, unsampled years, and health behaviors and outcomes is unknown. However, evidence suggests that the relationship between observed neighborhood physical disorder and health is likely mediated by perceptions of disorder, indicating that the concurrent validity correlations reported herein could motivate similar spatio-temporal studies with health behaviors and outcomes previously associated with observed neighborhood physical disorder (O'Brien et al., 2019).

5. Conclusions

It is feasible to construct a spatio-temporal model of observed

neighborhood physical disorder from virtually audited GSV street-scapes. Availability of GSV data within an urban U.S. county is spatio-temporally patterned, yet a spatio-temporal regression Kriging model displays reasonably high prediction accuracy. Observed neighborhood physical disorder appears more variable across space and relatively stable over time. However, correlations between perceived neighborhood physical disorder and model-predicted observed neighborhood physical disorder support the use of spatio-temporal regression Kriging to model neighborhood physical disorder, especially if predicting observed neighborhood physical disorder at locations measured with high spatial precision. Future studies using GSV's spatio-temporal data should collect larger, more diverse samples and investigate correlations with various health behaviors and outcomes related to neighborhood physical disorder.

Funding

This study was supported by funds from the NIH (K07CA222158, R01CA185623, P01CA151135, P30CA072720–5919; P30CA072720–5929, P30CA016056), the American Cancer Society (RSGT-07–291–01-CPHPS). The New Jersey State Cancer Registry, Cancer Epidemiology Services, New Jersey Department of Health, is funded by the Surveillance, Epidemiology and End Results (SEER) Program of the National Cancer Institute under contract HSN261201300021I and control No. N01-PC- 2013–00021, the National Program of Cancer Registries (NPCR), Centers for Disease Control and Prevention under grant NU5U58DP006279–02–00 as well as the State of New Jersey and the Rutgers Cancer Institute of New Jersey. This study's funding sponsors had no role in study design; collection, analysis, and interpretation of data; writing the report; nor the decision to submit the report for publication.

Supplementary materials

Supplementary material associated with this article can be found, in the online version, at doi:10.1016/j.sste.2022.100506.

References

- Bader, M.D.M., Mooney, S.J., Lee, Y.J., Sheehan, D., Neckerman, K.M., Rundle, A.G., Teitler, J.O., 2015. Development and deployment of the Computer Assisted Neighborhood Visual Assessment System (CANVAS) to measure health-related neighborhood conditions. *Health Place* 31, 163–172.
- Bader, M.D.M., Mooney, S.J., Rundle, A.G., 2016. Protecting Personally Identifiable Information When Using Online Geographic Tools for Public Health Research. *Am. J. Public Health* 106 (2), 206–208.
- Bandera, E.V., Demissie, K., Qin, B., Llanos, A.A., Lin, Y., Xu, B., Omilian, A.R., 2020. The Women's Circle of Health Follow-Up Study: a population-based longitudinal study of Black breast cancer survivors in New Jersey. *J. Cancer Survivorship* 1–16.
- Chum, A., O'Campo, P., Lachaud, J., Fink, N., Kirst, M., Nisenbaum, R., 2019. Evaluating same-source bias in the association between neighbourhood characteristics and depression in a community sample from Toronto, Canada. *Soc. Psychiatry Psychiatr. Epidemiol.* 54 (10), 1177–1187. <https://doi.org/10.1007/s00127-019-01718-6>.
- Curtis, J.W., Curtis, A., Mapes, J., Szell, A.B., Cinderich, A., 2013. Using google street view for systematic observation of the built environment: analysis of spatio-temporal instability of imagery dates. *Int J Health Geogr* 12 doi:Artn 53, 10.1186/1476-072x-12-53.
- Donaldson, K., 2013. How Big is Your Neighborhood? SEHSD Working Paper, U.S. Census Bureau. #FY2013-064.
- Entwisle, B., 2007. Putting people into place. *Demography* 44 (4), 687–703 doi:10.1353/dem.2007.0045.
- Environmental Systems Research, I., 2020. ArcGIS Desktop. Version 10.5. *Redlands, CA: Environmental Systems Research Institute.*
- Fry, D., Mooney, S.J., Rodriguez, D.A., Caiaffa, W.T., Lovasi, G.S., 2020. Assessing Google Street View Image Availability in Latin American Cities. *J. Urban Health* doi: 10.1007/s11524-019-00408-7Google, L. [Go back in time with Street View].
- Hoeben, E.M., Steenbeek, W., Pauwels, L.J., 2018. Measuring disorder: observer bias in systematic social observations at streets and neighborhoods. *J Quant Criminol* 34 (1), 221–249.
- Mooney, S.J., Bader, M.D.M., Lovasi, G.S., Teitler, J.O., Koenen, K.C., Aiello, A.E., Rundle, A.G., 2017. Street Audits to Measure Neighborhood Disorder: virtual or In-Person? *Am. J. Epidemiol.* 186 (3), 265–273. <https://doi.org/10.1093/aje/kwx004>.

- Nesoff, E.D., Milam, A.J., Barajas, C.B., Furr-Holden, C.D.M., 2020. Expanding tools for investigating neighborhood indicators of drug use and violence: validation of the NifEty for virtual street observation. *Prev. Sci.* 21 (2), 203–210.
- O'Brien, D.T., Farrell, C., Welsh, B.C., 2019. Broken (windows) theory: a meta-analysis of the evidence for the pathways from neighborhood disorder to resident health outcomes and behaviors. *Soc. Sci. Med.* 228, 272–292. <https://doi.org/10.1016/j.socscimed.2018.11.015>.
- Pebesma, E., Heuvelink, G., 2016. Spatio-temporal interpolation using gstat. *RFID Journal* 8 (1), 204–218.
- Plascak, J.J., Llanos, A.A.M., Qin, B., Chavali, L., Lin, Y., Pawlish, K.S., Bandera, E.V., 2020a. Visual cues of the built environment and perceived stress among a cohort of black breast cancer survivors. *Health Place* 67, 102498. <https://doi.org/10.1016/j.healthplace.2020.102498>.
- Plascak, J.J., Rundle, A.G., Babel, R.A., Llanos, A.A.M., LaBelle, C.M., Stroup, A.M., Mooney, S.J., 2020b. Drop-And-Spin Virtual Neighborhood Auditing: assessing Built Environment for Linkage to Health Studies. *Am. J. Prev. Med.* 58 (1), 152–160. <https://doi.org/10.1016/j.amepre.2019.08.032>.
- Plascak, J.J., Schootman, M., Rundle, A.G., Xing, C., Llanos, A.A.M., Stroup, A.M., Mooney, S.J., 2020c. Spatial predictive properties of built environment characteristics assessed by drop-and-spin virtual neighborhood auditing. *Int J Health Geogr* 19 (1), 21. <https://doi.org/10.1186/s12942-020-00213-5>.
- Pruitt, S.L., McQueen, A., Deshpande, A.D., Jeffe, D.B., Schootman, M., 2012. Mediators of the effect of neighborhood poverty on physical functioning among breast cancer survivors: a longitudinal study. *Cancer Causes Control.* 23 (9), 1529–1540.
- Remigio, R.V., Zulaika, G., Rabello, R.S., Bryan, J., Sheehan, D.M., Galea, S., Lovasi, G.S., 2019. A Local View of Informal Urban Environments: a Mobile Phone-Based Neighborhood Audit of Street-Level Factors in a Brazilian Informal Community. *J. Urban Health* 96 (4), 537–548. <https://doi.org/10.1007/s11524-019-00351-7>.
- Ross, C.E., Mirowsky, J., 1999. Disorder and decay the concept and measurement of perceived neighborhood disorder. *Urban Affairs Review* 34 (3), 412–432.
- Rzotkiewicz, A., Pearson, A.L., Dougherty, B.V., Shortridge, A., Wilson, N., 2018. Systematic review of the use of Google Street View in health research: major themes, strengths, weaknesses and possibilities for future research. *Health Place* 52, 240–246. <https://doi.org/10.1016/j.healthplace.2018.07.001>.
- Sampson, R.J., Raudenbush, S.W., 1999. Systematic social observation of public spaces: a new look at disorder in urban Neighborhoods 1. *Am. J. Sociol.* 105 (3), 603–651.
- Sas, I., 2014. *SAS/STAT 9.4 User's guide*: SAS Institute.
- South, E.C., Hohl, B.C., Kondo, M.C., MacDonald, J.M., Branas, C.C., 2018. Effect of Greening Vacant Land on Mental Health of Community-Dwelling Adults A Cluster Randomized Trial. *Jama Network Open* (3), 1 doi:ARTN e180298, 10.1001/jamanetworkopen.2018.0298.
- Tang, J., Long, Y., 2019. Measuring visual quality of street space and its temporal variation: methodology and its application in the Hutong area in Beijing. *Landsc. Urban Plan.* 191, 103436.
- Taylor, R.B., 2012. Defining neighborhoods in space and time. *Cityscape* 225–230.
- Team, R.C. (2013). R: a language and environment for statistical computing.
- Thissen, D. (2000). In H. Wainer & N.J. Dorans (Eds.), *Computerized Adaptive testing: a Primer* (2nd ed., pp. p. 159-184). Mahwah, N.J.: Lawrence Erlbaum Associates.
- Tucker, P., Gilliland, J., 2007. The effect of season and weather on physical activity: a systematic review. *Public Health* 121 (12), 909–922.